

# Effects of Errors on the Side-Lobe Level of a Low-Side-Lobe Array Antenna

JAMES K. HSIAO

*Electromagnetics Branch  
Radar Division*

June 29, 1981



**NAVAL RESEARCH LABORATORY**  
Washington, D.C.

Approved for public release; distribution unlimited.

SECURITY CLASSIFICATION OF THIS PAGE (When Data Entered)

REPORT DOCUMENTATION PAGE		READ INSTRUCTIONS BEFORE COMPLETING FORM
1. REPORT NUMBER NRL Report 8485	2. GOVT ACCESSION NO.	3. RECIPIENT'S CATALOG NUMBER
4. TITLE (and Subtitle) EFFECTS OF ERRORS ON THE SIDE-LOBE LEVEL OF A LOW-SIDE-LOBE ARRAY ANTENNA		5. TYPE OF REPORT & PERIOD COVERED Interim report on a continuing NRL problem.
		6. PERFORMING ORG. REPORT NUMBER
7. AUTHOR(s) James K. Hsiao		8. CONTRACT OR GRANT NUMBER(s)
9. PERFORMING ORGANIZATION NAME AND ADDRESS Naval Research Laboratory Washington, DC 20375		10. PROGRAM ELEMENT, PROJECT, TASK AREA & WORK UNIT NUMBERS 62721N; XF21-222-555; 53-0750-B-1
11. CONTROLLING OFFICE NAME AND ADDRESS Naval Electronics Systems Command Washington, DC 20360		12. REPORT DATE June 29, 1981
		13. NUMBER OF PAGES 24
14. MONITORING AGENCY NAME & ADDRESS (if different from Controlling Office)		15. SECURITY CLASS. (of this report) Unclassified
		15a. DECLASSIFICATION/DOWNGRADING SCHEDULE
16. DISTRIBUTION STATEMENT (of this Report)  Approved for public release; distribution unlimited.		
17. DISTRIBUTION STATEMENT (of the abstract entered in Block 20, if different from Report)		
18. SUPPLEMENTARY NOTES		
19. KEY WORDS (Continue on reverse side if necessary and identify by block number) Antenna Phased array Phased array error		
20. ABSTRACT (Continue on reverse side if necessary and identify by block number)  This report examines the effects of array errors on the side-lobe distribution of a phased array. The statistical distribution of this side-lobe level is shown to be Rician. A set of universal curves which give the cumulative probability of the percent deviation of side-lobe levels from the designed values is plotted. The variance, which is normalized with respect to the designed side-lobe level, is used as a parameter for this family of curves. This variance is a function of both the array errors and the illumination function. It is shown that the illumination function can be approximated by the number of array elements. Values of variance as a function of array error are also (Continued)		

DD FORM 1473  
1 JAN 73EDITION OF 1 NOV 65 IS OBSOLETE  
S/N 0102-014-6601

SECURITY CLASSIFICATION OF THIS PAGE (When Data Entered)

20. ABSTRACT (Continued)

plotted. With these curves, it is very easy to find the probability of the deterioration of the side-lobe level, if the array size and error distribution are known. The effect of correlated array error in a planar array is discussed. The variance due to this correlated error is a function of the array pattern of the subarray having this correlated error.

## CONTENTS

INTRODUCTION .....	1
STATISTICAL DISTRIBUTION OF ARRAY PATTERN .....	1
VALUES OF $\sigma_1$ AND $\sigma_2$ .....	4
STATISTICAL DISTRIBUTION OF SIDE-LOBE LEVEL .....	5
SIDE-LOBE REGION FOR $\mu = \pi$ .....	9
PLANAR ARRAYS WITH CORRELATED ERRORS .....	11
CONCLUSIONS .....	15
REFERENCES .....	15
Appendix A – DERIVATION OF VARIANCES FOR A LINEAR ARRAY .....	16
Appendix B – PROOF THAT THE ILLUMINATION FUNCTION IS BOUNDED .....	18
Appendix C – DERIVATION OF VARIANCES FOR A PLANAR ARRAY .....	19

## EFFECTS OF ERRORS ON THE SIDE-LOBE LEVEL OF A LOW-SIDE-LOBE ARRAY ANTENNA

### INTRODUCTION

Low-side-lobe array antennas have received wide interest in recent years. Theoretically, one can design an array antenna with any desired side-lobe level. However, in practice array errors and other imperfections limit the side-lobe level. One question is then how low a side-lobe level one may achieve in practice. This problem is essentially that of finding the effect of array errors on the array radiation pattern. This effect has been analyzed extensively in the literature. Ruzé [1] considered the effect on the radiation pattern of random errors in the exciting currents. Bailin and Ehrlich [2] treated the physical errors which cause the random errors in the exciting currents. Gilbert and Morgan [3] treated the effect on gain of random geometric errors in the general two-dimensional aperture. Elliot [4] further treated the problem of tolerance for two-dimensional scanning antennas. Allen et al. [5] reviewed the general problem; they did extensive study on all aspects of this problem.

In this report, the relationship between the side-lobe level and the array random errors will be examined. In particular, the limitation on the side-lobe level as a function of the array errors will be presented. Intuitively, one may see that this limitation must be a function of the desired side-lobe level, the number of elements in the array, and the nature of these errors. Since these errors are generally random in nature, the results are in terms of probability distributions. Allen et al. [5] showed that all array errors that result from feed, phase shifters, mechanical location, and the orientation of radiating elements can be characterized by a phase error and an amplitude error for each element in the array. The results of this study, therefore, are in terms of these errors. In the past, these errors have generally been assumed to be statistically independent. However, there are cases for which errors in many elements are not necessarily independent. For example, the same phase and amplitude in a row or column feed network could feed to every element in a particular row or column, or in the case of subarray configuration, the same error may propagate to every element in a particular subarray. These errors are correlated in these groups of elements. The effects of these correlated errors will be also discussed.

### STATISTICAL DISTRIBUTION OF ARRAY PATTERN

For simplification, linear arrays will be treated first. The array pattern of a linear array can be represented by

$$P(\theta) = \sum_n A_n \exp[-j(2\pi nd/\lambda)(\sin \theta - \sin \theta_0)], \quad (1)$$

where  $\theta$  is the angle of incidence of a plane wave on the array and  $\theta_0$  is the beam pointing angle. Element spacing  $d$  is assumed to be uniform. We further define

$$\mu = (2\pi d/\lambda)(\sin \theta - \sin \theta_0). \quad (2)$$

Equation (1) then becomes

$$P(\mu) = \sum_n A_n \exp(jn\mu). \quad (3)$$

For radiation in real space,  $\mu$  is constrained so that

$$|\mu| \leq 2\pi. \quad (4)$$

Due to mechanical and electrical errors in the array, the array pattern becomes

$$G(\mu) = \sum_n A_n (1 + \delta_n) \exp(j\phi_n) \exp(jn\mu), \quad (5)$$

where  $\delta_n$  is the amplitude error in percent and  $\phi_n$  is the phase error. These errors vary from element to element and are random in nature. For simplification, we assume that these errors have a known probability density function. Because of randomness of these errors,  $G(\mu)$  is a random complex function which is the sum of many random variables. Each of these random variables can be represented as

$$\begin{aligned} P_n(\mu) &= (1 + \delta_n) \exp(j\phi_n) \exp(jn\mu) \\ &= X_n + jY_n. \end{aligned} \quad (6)$$

These random variables are independent and have the same probability density function. The array pattern is hence a random function of the sum of many random variables, so that

$$\begin{aligned} G(\mu) &= g_1(\mu) + jg_2(\mu) \\ &= \sum_n A_n X_n + j \sum_n A_n Y_n. \end{aligned} \quad (7)$$

According to Lindenberg and Levy's central limit theorem [6],  $g_1(\mu)$  and  $g_2(\mu)$  are asymptotically normal. The means and variances of  $g_1(\mu)$  and  $g_2(\mu)$  are the weighted sums of means and variances of  $X_n$  and  $Y_n$ . The means of  $g_1(\mu)$  and  $g_2(\mu)$  are then respectively

$$\overline{g_1(\mu)} = \Phi(1) \sum_n A_n \cos n\mu \quad (8a)$$

and

$$\overline{g_2(\mu)} = \Phi(1) \sum_n A_n \sin n\mu, \quad (8b)$$

where  $\Phi(k)$  is the characteristic function of random variable  $x$ , defined as

$$\Phi(k) = \int g(x) \exp(jkx) dx,$$

where  $g(x)$  is the probability density function of random variable  $x$ . Furthermore, in deriving the above expression we have also assumed that the amplitude error  $\delta_n$  has zero mean. If the linear array is symmetrically illuminated, such that  $A_n = A_{-n}$ , then  $g_2(\mu) = 0$ . The variances of  $g_1(\mu)$  and  $g_2(\mu)$  are, respectively,

$$\sigma_1^2 = 1/2 \sum_n A_n^2 (A + B \cos 2n\mu) \quad (9a)$$

and

$$\sigma_2^2 = 1/2 \sum_n A_n^2 (A - B \cos 2n\mu), \quad (9b)$$

where

$$A = 1 + \sigma_\delta^2 - \Phi^2(1) \quad (9c)$$

and

$$B = (1 + \sigma_\delta^2)\Phi(2) - \Phi^2(1). \quad (9d)$$

The quantity  $\sigma_\delta^2$  is the variance of the amplitude error  $\delta$ . The covariance of  $g_1(\mu)$  and  $g_2(\mu)$  is

$$\sigma_{12} = 1/2 \sum_n A_n^2 B \sin 2n\mu. \quad (10)$$

For the symmetrically illuminated array,  $\sigma_{12}$  is zero. Derivations of these variances are included in Appendix A. The joint density function of the complex variable  $P(\mu)$  is

$$P[g_1(\mu), g_2(\mu)] = \frac{1}{2\pi\sqrt{\sigma_1\sigma_2}} \exp \left[ -\frac{(g_1 - \bar{g}_1)^2}{2\sigma_1^2} - \frac{g_2^2}{2\sigma_2^2} \right]. \quad (11)$$

The probability density function  $P(g_1, g_2)$  is a generalized noncentral chi-square distribution with two degrees of freedom. When  $\bar{g}_1 = 0$  and  $\sigma_1 = \sigma_2$ , this becomes a Rayleigh distribution. For the case  $\bar{g}_1 \neq 0$  and  $\sigma_1 = \sigma_2$ , it is sometimes referred to as a Rician distribution. Since the chi-square distribution cannot be evaluated in a straightforward way, we shall attempt to determine if it can be approximated.

The variances  $\sigma_1$  and  $\sigma_2$ , as shown in Eqs. (9a) and (9b), consist of two parts. The first part is

$$p_1 = 1/2 A \sum_n A_n^2, \quad (12a)$$

and the second part is

$$p_2 = 1/2 B \sum_n A_n^2 \cos 2n\mu. \quad (12b)$$

The first part is not a function of  $\mu$ , but the second part is. Since  $p_2$  is the sum of cosine functions except at regions in the vicinity of  $\mu = k\pi$ ,  $p_1$  is much greater than  $p_2$ . An example is shown in Fig. 1, on which two sets of curves are shown. Curve 1 shows the  $\sigma_1$  and  $\sigma_2$  values as a function of  $\mu$  for the case of a 20-element, 30-dB Chebyshev array. The amplitude error has a variance of 10%, and the phase error has a normal distribution with zero mean and a  $5^\circ$  variance. One may see that the variances are independent of  $\mu$  and  $\sigma_1 = \sigma_2$  except in the regions at  $\mu = \pi$  and  $\mu = 2\pi$ . Curve 2 on this figure shows the case of an 80-element Chebyshev array with 50-dB side lobe design, an amplitude error of 0.005, and a phase error of  $2^\circ$  rms. Note that  $\sigma_1$  and  $\sigma_2$  of curve 2 are considerably smaller than those of curve 1. This is because there are more elements and a smaller error in the case of curve 2. This will be discussed in more detail later. From this, one may conclude that in the side-lobe region where  $\mu \neq \pi$  one may assume that  $\sigma_1 = \sigma_2 = p_1$ . The chi-square probability density of Eq. (11) then becomes Rician, and

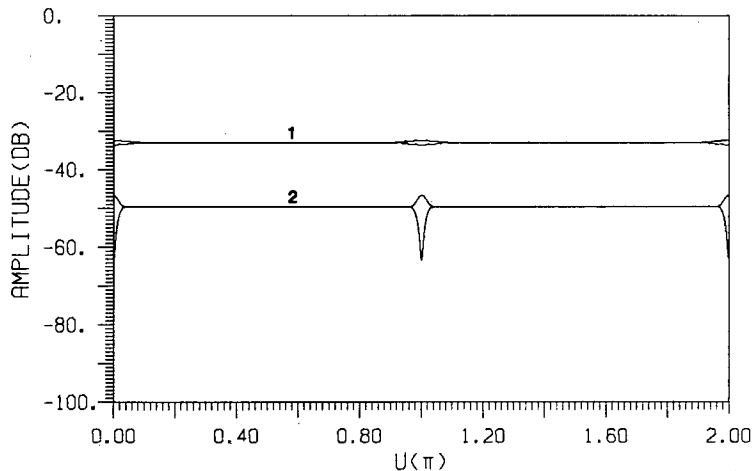


Fig. 1 - Values of  $\sigma_1$  and  $\sigma_2$  (case 1: 20 element Chebyshev, 30 dB,  $\sigma_a = 0.1$ ,  $\sigma_\phi = 5^\circ$ ; case 2: 80 element Chebyshev, 50 dB,  $\sigma_a = 0.005$ ,  $\sigma_\phi = 2^\circ$ )

$$P(R) = \frac{R}{\sigma^2} \exp [-(R - \bar{g}_1)^2] I_0 \left( \frac{R\bar{g}_1}{\sigma^2} \right), \quad (13)$$

where  $R = \sqrt{g_1^2 + g_2^2}$  is the amplitude of the radiation pattern and  $I_0(z)$  is the modified Bessel function of zero order.

Radiation in regions in the vicinity of  $\mu = k\pi$ , which contain the main-beam and grating-lobe regions and a small portion of the side-lobe region, has essentially a chi-square statistical distribution as shown in Eq. (11).

Before further discussing the radiation level statistic, let us examine  $\sigma_1$  and  $\sigma_2$  more carefully.

#### VALUES OF $\sigma_1$ AND $\sigma_2$

In the vicinity of  $\mu = k\pi$ ,  $\sigma_1$  and  $\sigma_2$  can be approximated by

$$\sigma_1^2 \approx 1/2 (A + B) \sum_n A_n^2 \quad (14a)$$

and

$$\sigma_2^2 \approx 1/2 (A - B) \sum_n A_n^2, \quad (14b)$$

and in other sidelobe regions one has

$$\sigma_1^2 \approx \sigma_2^2 = A \sum_n A_n^2. \quad (14c)$$

Each  $\sigma$  consists of two parts. The first part is  $\sum_n A_n^2$ , which is a function of the number of elements in the array and the illumination function of the array. The second part is  $A$ ,  $A - B$ , or  $A + B$  and is a function of the parameters  $A$  and  $B$  given in Eqs. (9c) and (9d), which are determined by random array errors.

In finding the first part of  $\sigma$ , for convenience of comparison, let us normalize the array illumination function  $A_n$  in such a way that

$$\sum A_n = 1. \quad (15)$$

This implies that at the peak of the main beam the radiated field has unit strength (or zero dB). The summation of  $A_n^2$  is then always less than unity. In the case of a uniformly illuminated array,

$$\sum_n A_n^2 = \frac{1}{N}, \quad (16)$$

where  $N$  is the total number of antenna elements. In Appendix B it is shown that no matter how the illumination function is formed the  $1/N$  factor is its lower bound; in other words,

$$\sum_n A_n^2 \geq \frac{1}{N}. \quad (17)$$

Figure 2 shows some examples of  $\sum_n A_n^2$  for a Chebyshev array. It is evident that in all the different designs the  $\sum_n A_n^2$  is close to the factor  $1/N$  and it is always bounded by this factor. This is useful for the estimation of  $\sigma$ . One may replace  $\sum_n A_n^2$  by the inverse of the number of elements in the array for a first-order estimation.

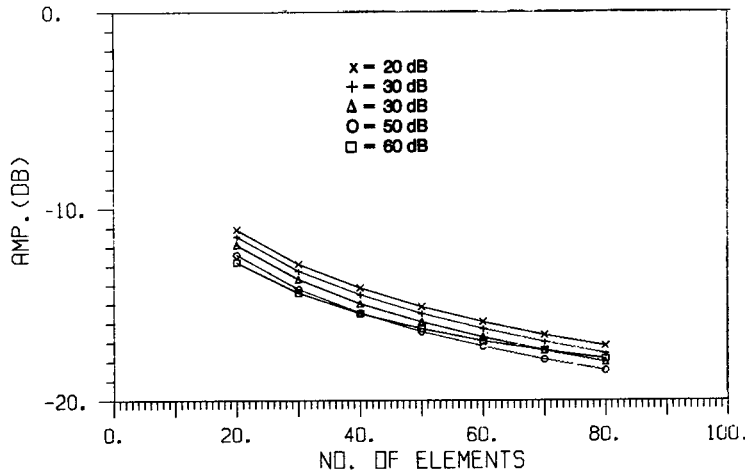


Fig. 2 — Values of  $\sum_n A_n^2$  for a Chebyshev array with different side-lobe levels

In finding the second part of  $\sigma$ , we consider the phase error. The probability density function of the phase error  $\phi$  is an even function with zero mean; hence  $\Phi(k)$  is real. Furthermore, in most cases of interest, the probability function is most likely concentrated in a very small angle region (less than  $\pm \pi/2$ ). In this case  $\Phi(1)$  and  $\Phi(2)$  would be positive and

$$\Phi(k) \leq \Phi(0) = 1.$$

When the phase error probability density is an impulse function centered at zero degrees, both  $\Phi(1)$  and  $\Phi(2)$  are equal to unity. Under this condition  $A = B = \sigma_\phi^2$ , the variance of the amplitude error. As the phase error increases, the probability density function  $p(\phi)$  spreads out and  $\Phi(k)$  is less than unity; parameter  $A$  then increases monotonically as the phase error increases. This is shown in Figs. 3a and 3b. Figure 3a shows the case for which the phase error density function is normal; Fig. 3b shows the case for a uniform density function. In the side-lobe region,  $\sigma = A \sum_n A_n$ ; one may therefore estimate the value very easily by multiplying this factor by  $1/N$ . Some typical values of the parameter  $B$  are shown in Figs. 4a and 4b for normal and uniform angle error density functions, respectively.

### STATISTICAL DISTRIBUTION OF SIDE-LOBE LEVEL

In the main-beam region where  $\mu \approx 0$  and  $\sigma_1 \neq \sigma_2$ , the radiation level has a noncentral chi-square density function. For this type of density function most of the probability mass concentrates within an ellipse with major and minor semiaxes of two to three times  $\sigma_1$  and  $\sigma_2$ , centered at the mean value  $\bar{g}_1$ . Furthermore,

$$\bar{g}_1 \gg \sigma_1 \text{ or } \sigma_2.$$

Therefore, for practical purposes one may assume that the radiation amplitude ( $R_0 = \sqrt{g_1^2 + g_2^2}$ ), is equal to  $\bar{g}_1$  with a probability of unity,

$$R_0 \approx \bar{g}_1 = \Phi(1) \sum_n A_n.$$

Since the illumination function  $A_n$  is normalized, one finds

$$R_0 \approx \Phi(1). \tag{18}$$

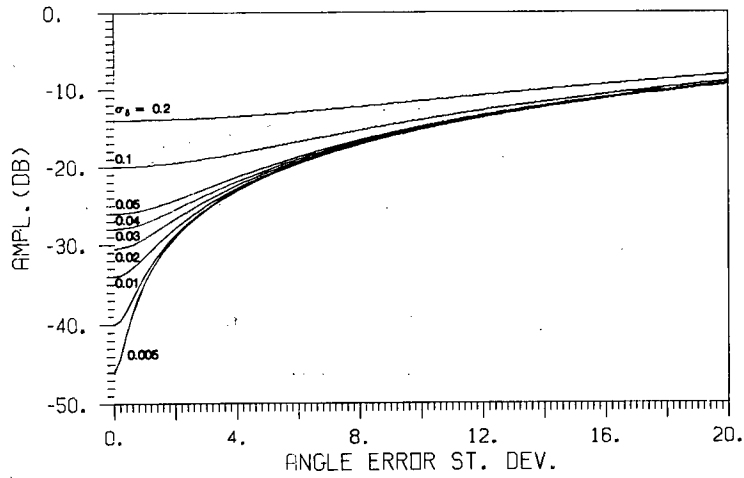


Fig. 3(a) — Values of A: phase error has a normal distribution

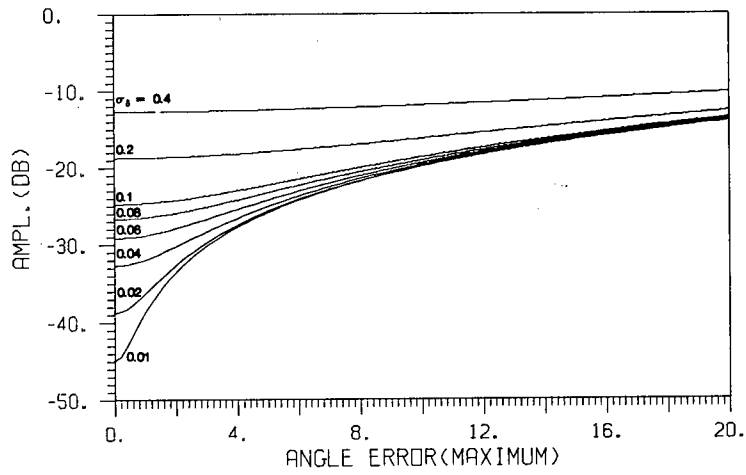


Fig. 3(b) — Values of A: phase error has a uniform distribution

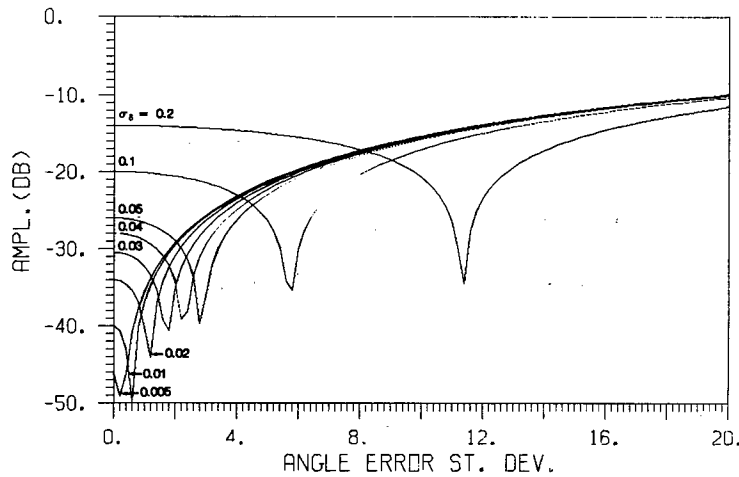


Fig. 4(a) — Values of B: angle error has a normal distribution

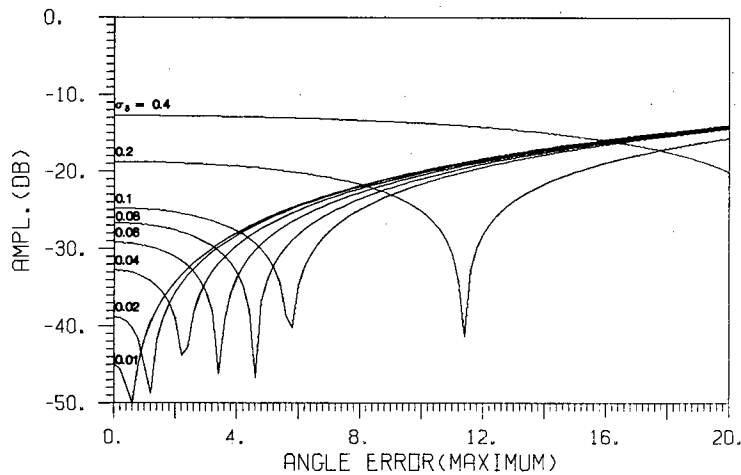


Fig. 4(b) — Values of B: angle error has a uniform distribution

In the side-lobe region, there are cases in which  $\mu = \pi$  and in which  $\mu \neq \pi$ . Since the region in the vicinity of  $\mu = \pi$  is limited to about one beamwidth, we shall first examine the case for  $\mu \neq \pi$ .

The probability density function in the side-lobe region where  $\mu \neq \pi$  has a Rician distribution. The side-lobe level is defined as the ratio of the main-beam level to the side-lobe level. Its probability function is the joint probability function of  $R_0$  and  $R$ . Since we showed earlier that  $R_0 \approx \Phi(1)$  with a probability of unity, the probability density function of the ratio of  $R$  to  $R_0$  is the same as that of  $R$  with a scale factor  $\Phi(1)$ ; that is,  $R' = R/\Phi(1)$ , and the density function of  $R'$  is then

$$P(R') = \frac{R'}{\sigma^2} \exp \left\{ \left( [R'\Phi(1)]^2 - \bar{g}_1^2 \right) / 2\sigma^2 \right\} I_0 \left[ \frac{R'\Phi(1)\bar{g}_1}{\sigma^2} \right], \quad (19)$$

where

$$\sigma = \sigma_1 = \sigma_2$$

and

$$\bar{g}_1 = \Phi(1) \sum_n A_n \cos n\mu.$$

For convenience, we shall normalize this  $R'$  in such a way that

$$P(S) = \frac{S}{\sigma'^2} \exp \left[ -\frac{S^2 + 1}{2\sigma'^2} \right] I_0 \left[ \frac{S}{\sigma'^2} \right], \quad (20)$$

where

$$S = R' / \sum_n A_n \cos n\mu \quad (21a)$$

and

$$\sigma' = \sigma / \left( \sum_n A_n \cos n\mu \right). \quad (21b)$$

We notice that  $\sum_n A_n \cos n\mu$  represents the side-lobe level at the angle  $\mu$  when there is no error present. Therefore, both  $S$  and  $\sigma'$  in this equation are measured in terms of the designed side-lobe level. This is more convenient to use than are values in terms of  $\sigma$  or  $\bar{g}_1$ .

The cumulative probability of  $S$  being less than  $S_L$  is then

$$P(S < S_L) = \int_0^{S_L} \frac{S}{\sigma'^2} \exp \left[ -\frac{S^2 + 1}{2\sigma'^2} \right] I_0 \left[ \frac{S}{\sigma'^2} \right] dS. \quad (22)$$

A family of such curves with  $\sigma'$  as parameter is shown in Fig. 5. Each of these curves presents the cumulative probability that  $S$  (in terms of designed side lobe) is less than or equal to a level  $S_L$  for a given  $\sigma'$ . Since this curve is presented in such a way that it is not a function of the angle  $\mu$ , these curves apply to all points in the side-lobe region. Secondly, these curves are normalized with respect to the ideal side-lobe level. It represents the probability of the deviation of side-lobe level from the designed value. Although they are not presented explicitly as a function of  $\mu$ , they are related to the side-lobe level. For example, at the peak of a side lobe, the normalized  $\sigma'$  may be only equal to 0.1, but at a point where the side-lobe level may be 10 times smaller, the normalized  $\sigma'$  then becomes 10 times larger. One can see the difference in the probability distribution for these two cases. This set of curves is universal. It applies to arrays with different illumination designs, different sizes, and different errors.

With the aid of this plot, one may easily determine the required error tolerance to achieve a desired side-lobe level. For example, one may wish to design an array having a 50-dB side-lobe, with probability of 90% that the side-lobe level will not exceed the designed level by more than 30%. The curve for  $\sigma' = 0.2$  satisfies this condition, because for  $S = 1.3$  the cumulative probability is 90%. Since  $\sigma' = 0.2$  is equivalent to -14 dB, the required  $\sigma^2$  is approximately 64 dB (50+14). Suppose that the array has 100 elements. This value of  $N$  gives at best 20 dB; one therefore needs an error level that would yield no less than 44 dB. From Fig. (3a), one sees that an amplitude error of 0.5% ( $1\sigma$ ) and an angle error of  $1.5^\circ$  ( $1\sigma$ ) will satisfy this requirement.

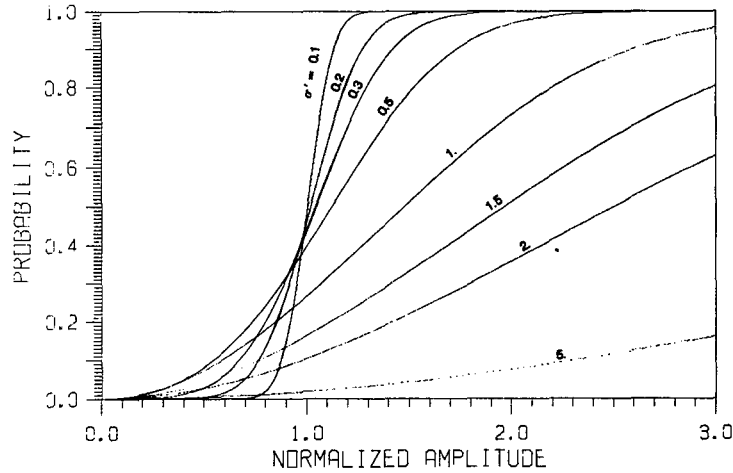


Fig. 5 — Cumulative probability distribution of normalized side-lobe level (normalized to the designed value)

The validity of the curves shown in Fig. 5 has been checked by means of computer simulation. In this simulation, we first computed the probability curve as shown in Fig. 5 for an array of 52 elements with a 50-dB side-lobe design with given phase and amplitude statistical error distributions. The results are plotted in Fig. 6. Next, we computed the side lobe level of this array about 10,000 times. Each time the actual phase and amplitude for each element of the array was generated by the random-number generator according to the prescribed distribution. These phase and amplitude errors were then added to each element in the array. Pattern values were computed in the side-lobe region and normalized to the designed side-lobe level. The statistical distribution of these computations is plotted in Fig. 6 with crosses, and the theoretical curve is also plotted. One may see that these two results closely coincide.

#### SIDE-LOBE REGION FOR $\mu = \pi$

In the side-lobe region where  $\mu = \pi$ ,  $\sigma_1 \neq \sigma_2$ , and the probability density function of the radiation pattern becomes a noncentral chi-square distribution similar to that in the main-beam region. The relationship that  $\bar{g}_1 \gg \sigma_1$  and  $\sigma_2$  does not hold; therefore, the approximation used in the main-beam region cannot be applied. Because the region in the vicinity of  $\mu = \pi$  is very small (about one beamwidth), it has been ignored in the past. However, it is worthwhile to investigate the probability that an undesired high side-lobe may appear in this area.

It was pointed out earlier that most of the probability mass of a noncentral chi-square distribution concentrates within an ellipse with major and minor semi-axes of two times  $\sigma_1$  and  $\sigma_2$ , centered at the mean value  $\bar{g}_1$ . This situation is depicted in Fig. 7. When  $\sigma_1 \approx \sigma_2$ , the maximum value of  $R$  is

$$R_{\max} = \sqrt{\bar{g}_1^2 + (2\sigma_2)^2}, \tag{23}$$

and when  $\sigma_2 \ll \sigma_1$

$$R_{\max} = \bar{g}_1 + 2\sigma_1. \tag{24}$$

This  $R_{\max}$  is the maximum side-lobe level, with a very high probability that no side-lobe level will exceed this value. When  $\bar{g}_1 > \sigma_1$  or  $\sigma_2$ , the difference between values of  $R_{\max}$  in Eqs. (23) and (24) is very small. Thus for cases which have a very high probability of a small deviation of the side lobe from the designed value, the approximation of the noncritical chi-square distribution with a Rician distribution is acceptable.

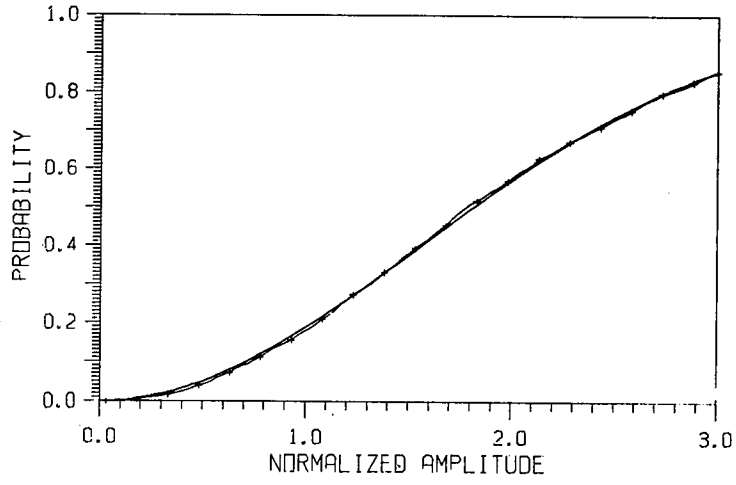


Fig. 6 — Simulation result (curve with crosses) compared to a theoretical result

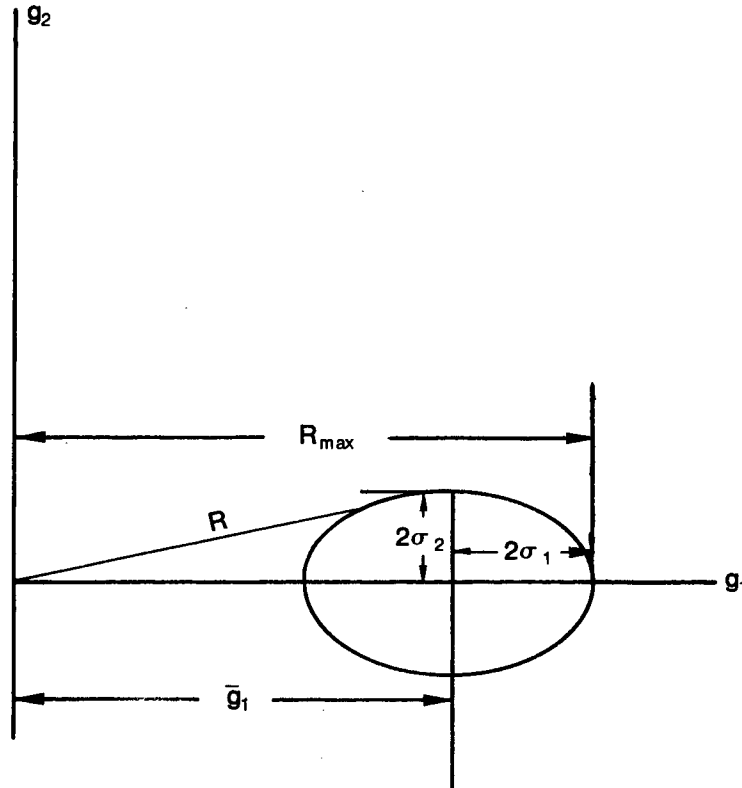


Fig. 7 — Probability distribution in region  $\mu = \pi$  or  $2\pi$

In this region, from Eqs. (9a) and (9b),

$$\sigma_1^2 \approx \frac{1}{2} (A + B) \sum_n A_n^2 \quad (25a)$$

and

$$\sigma_2^2 \approx \frac{1}{2} (A - B) \sum_n A_n, \quad (25b)$$

where  $A$  and  $B$  are functions of the characteristic function of phase error and the standard deviation of amplitude error as shown in Eqs. (9c) and (9d). For a very small phase error both  $\Phi(1)$  and  $\Phi(2)$  are close to unity, hence  $A \approx B$ ,  $\sigma_1 \approx 2A$ , and  $\sigma_2 \approx 0$ . As the phase error increases,  $A$  increases and  $B$  decreases. One may see this from Figs. 3a and 4a (or Figs. 3b and 4b). In this case, one may assume that  $B = 0$  and  $\sigma_1 = \sigma_2 = A$ . The maximum side-lobe levels with a high probability for these two cases are, respectively,

$$R_{\max} = \bar{g}_1 + 4A \quad (26a)$$

and

$$R_{\max} = \bar{g}_1 + 2A. \quad (26b)$$

One may see this intuitively. When the phase error is zero, amplitude errors have a good chance to line up and induce a higher side-lobe level. On the other hand, if phase errors are introduced the chance of all amplitude errors to be lined up in the same direction is greatly reduced, hence the  $R_{\max}$  value has a higher probability of being smaller. If the phase error is further increased, eventually  $A \approx -B$ . In this case  $\sigma_1 = 0$  and  $\sigma_2 = 2A$ , and under this condition

$$R_{\max} = \sqrt{\bar{g}_1^2 + (4A)^2}. \quad (27)$$

This  $R_{\max}$  value is slightly greater than the one in Eq. (26b). This is the case in which phase errors are so great that the imaging component dominates and it has a good chance to be lined up and introduces a higher amplitude error. However, if  $\bar{g}_1 \gg A$ , the error introduced by the approximation  $\sigma_1 = \sigma_2 = A$  is small. This is shown in Fig. 8. Curve 1 is the cumulative probability of the normalized amplitude for  $\sigma_1 = \sigma_2$  with the normalized  $\sigma_1 = 0.1$ ; curve 2 is for the case  $\sigma_1 = 0.199$  and  $\sigma_2 = 0.0001$ ; and curve 3 is for the case  $\sigma_1 = 0.0001$  and  $\sigma_2 = 0.199$ . The difference in the probability distribution of these three cases is negligible for practical purposes.

## PLANAR ARRAYS WITH CORRELATED ERRORS

For a planar array, if errors in each element are independent, the results of the linear array can be applied directly. The array pattern of a planar array with independent errors can be represented by

$$G(\mu, \nu) = \sum_n \sum_m A_{nm} (1 + \delta_{nm}) \exp(j\phi_{nm}) \exp[j(m\mu + n\nu)], \quad (28)$$

where

$$\mu = (2\pi d_x/\lambda) (\sin \theta \cos \phi - \sin \theta_0 \cos \phi_0),$$

$$\nu = (2\pi d_y/\lambda) (\sin \theta \sin \phi - \sin \theta_0 \sin \phi_0),$$

and  $\delta_{nm}$  and  $\phi_{nm}$  are the amplitude and phase errors respectively. It can be shown that the  $\sigma_1$  and  $\sigma_2$  of this case are given by

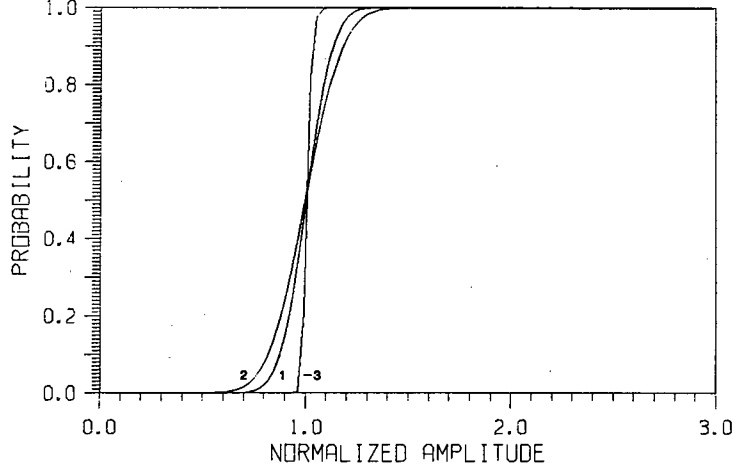


Fig. 8 — Probability distribution at region  $\mu = \pi, \sigma = 0.1$

$$\sigma_1^2 = \frac{1}{2} \sum_n \sum_m [C_{nm} + D_{nm} \cos(2m\mu + 2n\nu)], \quad (29a)$$

$$\sigma_2^2 = \frac{1}{2} \sum_n \sum_m [C_{nm} - D_{nm} \cos(2m\mu + 2n\nu)], \quad (29b)$$

where

$$C_{nm} = [1 + \sigma_{nm}^2 - \Phi_{nm}^2(1)] A_{nm}^2 \quad (29c)$$

and

$$D_{nm} = [(1 + \sigma_{nm}^2) \Phi_{nm}(2) - \Phi_{nm}^2(1)] A_{nm}^2, \quad (29d)$$

and

$$\sigma_{12} = \frac{1}{2} \sum_n \sum_m [(1 + \sigma_{nm}^2) \Phi_{nm}(2) - \Phi_{nm}^2(1)] A_{nm}^2 \sin(2m\mu + 2n\nu). \quad (30)$$

Comparing these equations with Eqs. (9a), (9b), and (10) one may see that they are almost identical. Therefore, all results obtained for the linear array can be applied directly. Since a planar array usually has more elements than a linear array,  $\sigma_1$  and  $\sigma_2$  in general are smaller. It therefore can tolerate larger errors with less degradation. Unfortunately, in most cases errors in each element are not independent. They may be correlated. For example, a planar array may be fed by rows and columns. The same error from the feed network may appear in every element in an entire row (or column) or in many cases all elements of a subarray may contain the same error due to mechanical reasons. To examine this effect, we shall first examine a case for which the same error appears in every element of a row (or column) in an array. Besides this correlated error, there are also independent errors in every element. The array pattern can then be assumed to have the following form:

$$G(\mu, \nu) = \sum_n (1 + \delta_n) \exp(j\phi_n) \sum_m A_{nm} (1 + \delta_{nm}) \exp(j\phi_{nm}) \exp[j(m\mu + n\nu)], \quad (31)$$

where  $\delta_n$  and  $\phi_n$  are, respectively, the amplitude and phase errors which appear in the  $n$ th row. Appendix C shows that

$$\sigma_1^2 = E + F \quad (32a)$$

and

$$\sigma_2^2 = E - F, \quad (32b)$$

where

$$E = \frac{1}{2} \sum_n \sum_m [(1 + \sigma_n^2) (1 + \sigma_{nm}^2) - \Phi_n^2(1) \Phi_{nm}^2(1)] A_{nm}^2 + \frac{1}{2} \sum_n [(1 + \sigma_n^2) - \Phi_n^2(1)] \Phi_{nm}^2(1) \sum_m \sum_s A_{nm} A_{ns} \cos(m-s)\mu \quad (32c)$$

and

$$F = \frac{1}{2} \sum_n \sum_m [(1 + \sigma_n^2) (1 + \sigma_{nm}^2) \Phi_n(2) \Phi_{nm}(2) - \Phi_n^2(1) \Phi_{nm}^2(1)] \cdot A_{nm}^2 \cos(2m\mu + 2n\nu) + \frac{1}{2} \sum_n \sum_m \sum_s [(1 + \sigma_n^2) \Phi_n(2) - \Phi_n^2(1)] \cdot \Phi_{nm}^2(1) A_{nm} A_{ns} \cos[(m+s)\mu + 2n\nu]. \quad (32d)$$

In the derivation of Eqs. (32), it is assumed that the amplitude errors  $\delta_n$  and  $\delta_{nm}$  have zero mean and their respective variances are  $\sigma_n^2$  and  $\sigma_{nm}^2$ . In the formulation, we also assumed that the amplitude error consists of two levels  $\delta_n$  and  $\delta_{nm}$ , and the total error is  $(1 + \delta_n) (1 + \delta_{nm})$ . The mean of this error is zero; however, the composite variance is given by

$$(1 + \sigma_n^2) (1 + \sigma_{nm}^2) = 1 + \sigma_n^2 + \sigma_{nm}^2 + \sigma_n^2 \sigma_{nm}^2. \quad (33)$$

Let the total amplitude variance  $\sigma$  be given by

$$\sigma^2 = \sigma_n^2 + \sigma_{nm}^2 + \sigma_n^2 \sigma_{nm}^2. \quad (34)$$

If both  $\sigma_n$  and  $\sigma_{nm}$  are small, the total variance  $\sigma^2$  can be viewed as the sum of the individual variances  $\sigma_n^2$  and  $\sigma_{nm}^2$ . Let the total phase error  $\phi$  be the sum of the two phase errors  $\phi_n$  and  $\phi_{nm}$ , then the characteristic function of  $\Phi$  is

$$\Phi = \Phi_n(1) \Phi_{nm}(1). \quad (35)$$

Equations (32a) and (32b) consist of two parts, similar to Eqs. (9a) and (9b) in the case of a linear array. The terms which involve  $\cos(2m\mu + 2n\nu)$  and  $\cos[(m+s)\mu + 2n\nu]$  can be ignored except perhaps in regions very close to the main beam and where  $2m\mu + 2n\nu$  and  $(m+s)\mu + 2n\nu$  are integer multiples of  $2\pi$ . These regions are only one beamwidth in extent, and their effect may be ignored for the same reason that was used in the case of a linear array. We hence have

$$\sigma_1^2 = \sigma_2^2 = \frac{1}{2} \sum_n \sum_m [1 + \sigma^2 - \Phi^2(1)] A_{nm}^2 + \frac{1}{2} \sum_n [(1 + \sigma_n^2 - \Phi_n^2(1)) |G_n(\mu)|^2, \quad (36)$$

where

$$|G_n|^2 = \Phi_{nm}^2(1) \sum_m \sum_s A_{nm} A_{ns} \cos(m-s)\mu, \quad (37)$$

and  $\sigma_n$ ,  $\sigma_{nm}$ ,  $\Phi_n$ , and  $\Phi_{nm}$  are replaced by  $\sigma$  and  $\Phi$  as shown in Eqs. (34) and (35).

The mean radiation pattern of the linear array of the  $n$ th row is

$$G(\mu) = \Phi_{nm}(1) \sum_m A_{nm} \exp(jm\mu), \quad (38)$$

therefore  $|G(\mu)|^2$  is its power pattern. The  $\sigma_1$  and  $\sigma_2$  consist of two parts. The first part,  $\frac{1}{2} \sum_n \sum_m [1 + \sigma^2 - \Phi^2(1)] A_{nm}^2$ , is identical to that of an array with uncorrelated errors when both the correlated

and uncorrelated errors in each element are taken into account. The second portion,  $\frac{1}{2} \sum_n [(1 + \sigma_n^2 - \Phi_n^2(1))] |G(\mu)|^2$ , has a value similar to that of a linear array with the illumination weights  $A_n^2$  replaced by the power radiation pattern function  $|G(\mu)|^2$ . It is interesting to note that when  $\mu = 0$ ,  $|G(\mu)|^2$  has its maximum value. In other words, at  $\mu = 0$  the correlated errors have the strongest effect on  $\sigma$  and the array patterns would most probably deteriorate more at  $\mu = 0$  in the  $\mu, \nu$  domain. For example, a column and row fed array, as discussed in this section, has rows in the  $x$  direction and columns in the  $y$  direction. Elements in each column have a common error. If the array beam is steered at the broadside ( $\theta_0 = 0$ ), then  $\mu = \sin \theta \cos \phi$ , and the maximum degradation will occur in a plane along the  $y$  direction (the **E** plane), when  $\phi = 90^\circ$ . However, if elements in each row have a common error, the worst degradation may occur at  $\nu = 0$ , along the  $x$  direction (the **H** plane). Under this condition,

$$|G_m(\mu)|^2 = \sum_n \left( \sum_m A_{nm} \right)^2. \quad (39)$$

If the illumination coefficient  $A_{nm}$  values are normalized such that

$$\sum_n \sum_m A_{nm} = 1, \quad (40)$$

one can show that

$$|G_m(\mu)|^2 \geq \frac{1}{N}, \quad (41)$$

where  $N$  is the total number of rows which have correlated errors. One may hence conclude that:

- $\sigma_1 = \sigma_2$ .
- Both  $\sigma_1$  and  $\sigma_2$  consist of two parts, with the first part due to total errors (including both correlated and uncorrelated) at each array element ( $\sigma_\mu$ ) and the second part due to the correlated error fed to each row (or column) ( $\sigma_c$ ). The  $\sigma$  is the root sum square (RSS) of these two parts.
- Both  $\sigma_\mu$  and  $\sigma_c$  are functions of both the array element errors and the illuminations. The effects of amplitude and phase errors on the  $\sigma$  value are identical to that of the case of a linear array. Curves shown on Figs. 3a and 3b can be used to estimate this value. The array illumination can be approximated by the number of elements in the array (for  $\sigma_\mu$ ) and the number of rows (for  $\sigma_c$ ) for the correlated errors.

The covariance  $\sigma_{12}$  between real and imaginary parts of the array pattern is

$$\begin{aligned} \sigma_{12} = & \frac{1}{2} \sum_n \sum_m [(1 + \sigma_n^2) (1 + \sigma_{nm}^2) \Phi_n(2) \Phi_{nm}(2) - \Phi_n^2(1) \Phi_{nm}^2(1)] A_{nm}^2 \sin(2m\mu + 2n\nu) \\ & + \frac{1}{2} \sum_n \sum_m \sum_s [(1 + \sigma_n^2) \Phi_n(2) - \Phi_n^2(1)] \Phi_{nm}^2 A_{nm} A_{ms} \sin[(m+s)\mu + 2n\nu]. \end{aligned} \quad (42)$$

When the array is symmetrically illuminated and the phase center of the array is taken at the center of the array, one may show that  $\sigma_{12} = 0$ . Therefore, the distribution of array patterns of a planar array is Rician as shown in Fig. 5. The value of  $\sigma$  is the RSS of  $\sigma_\mu$  and  $\sigma_c$ . The above results can be applied to an array which is fed by subarrays and the correlated error appears in each subarray. In this case, one has to replace the parameters  $\mu$  and  $\nu$  with functions of  $\mu$  and  $\nu$ .

## CONCLUSIONS

In this report, we have shown the following:

1. The amplitude distribution of the radiation pattern for both a linear array and a planar array is Rician. A set of universal curves for such distributions is shown on Fig. 5. The curves are presented for different  $\sigma$  values and are normalized to the mean pattern value. They thus read directly in terms of cumulative probability of the degradation of the side-lobe level.

2. The  $\sigma$  value for both linear arrays and planar arrays has a similar form, which is a function of errors and array illuminations. The effect of errors is plotted in Fig. 3 for different error distributions. Figure 3 also shows that the illumination function of the array can be approximated by the number of elements.

3. For a planar array with correlated errors the variance  $\sigma$  is the RSS of  $\sigma_\mu$  and  $\sigma_c$ . The variance  $\sigma_\mu$  takes into account the error in each element (including both correlated and uncorrelated errors) and  $\sigma_c$  is due to the contribution of correlated error in a subarray. Both  $\sigma_\mu$  and  $\sigma_c$  are functions of the errors and the illuminations. However,  $\sigma_c$  is also a function of the subarray pattern in which the errors are correlated.

## REFERENCES

1. J. Ruze, "The Effect of Aperture Errors on the Antenna Radiation Pattern," *Supplemento Nuovo Cimento* **9**, 364-380 (1952).
2. L.L. Bailin and M.J. Ehrlich, "Factors Affecting the Performance of Linear Arrays," *Proc. IRE* **41**, 235-241 (Feb. 1953).
3. E.N. Gilbert and S.P. Morgan, "Optimum Design of Directive Antenna Arrays Subject to Random Variations," *Bell Syst. Tech. J.* **34**, 637-663 (May 1955).
4. R.S. Elliott, "Mechanical and Electrical Tolerance for Two-Dimensional Scanning Antenna Arrays," *IRE Trans. Antennas Propag.* **AP-6**, 114-120 (Jan. 1958).
5. J.L. Allen et al., "Phased Array Radar Studies," Technical Report No. 236, MIT Lincoln Laboratory, Nov. 1961.
6. Harald Cramér, *Mathematical Methods of Statistics*, Princeton University Press, Princeton, N.J., 1946, p. 45.

**Appendix A**  
**DERIVATION OF VARIANCES FOR A LINEAR ARRAY**

Define a complex random variable

$$z = x + jy; \quad (\text{A1})$$

then

$$E\{|z - E(z)|^2\} = \sigma_x^2 + \sigma_y^2, \quad (\text{A2})$$

where

$$\sigma_x^2 = E\{|x - E(x)|^2\}, \quad (\text{A3})$$

$$\sigma_y^2 = E\{|y - E(y)|^2\}, \quad (\text{A4})$$

and

$$E\{|z - E(z)|^2\} = \sigma_x^2 - \sigma_y^2 + 2j\sigma_{12}, \quad (\text{A5})$$

where

$$\sigma_{12} = E\{|x - E(x)\} [y - E(y)]\}. \quad (\text{A6})$$

Solving Eqs. (A5) and (A2), one gets

$$2\sigma_x^2 = E\{|z - E(z)|^2\} + \text{Re } E\{|z - E(z)|^2\}, \quad (\text{A7})$$

$$2\sigma_y^2 = E\{|z - E(z)|^2\} - \text{Re } E\{|z - E(z)|^2\}, \quad (\text{A8})$$

and

$$2\sigma_{12} = \text{Im } E\{|z - E(z)|^2\}. \quad (\text{A9})$$

For a linear antenna, the pattern function is

$$G(\mu) = \sum_n A_n (1 + \delta_n) e^{j\phi_n} e^{jn\mu}, \quad (\text{A10})$$

$$E(G) = \Phi(1) \sum_n A_n e^{jn\mu}, \quad (\text{A11})$$

$$|E(G)|^2 = \Phi^2(1) \sum_n \sum_m A_n A_m e^{j(n-m)\mu}, \quad (\text{A12})$$

$$[E(G)]^2 = \Phi^2(1) \sum_n \sum_m A_n A_m e^{j(n+m)\mu}, \quad (\text{A13})$$

$$E\{|G|^2\} = \sum_{\substack{n,m \\ n \neq m}} A_n A_m \Phi^2(1) e^{j(n-m)\mu} + \sum_n A_n^2 (1 + \sigma^2), \quad (\text{A14})$$

where  $\sigma^2$  is the variance of the amplitude error  $\delta_n$ ,

$$\begin{aligned} E\{|G - E(G)|^2\} &= E\{|z|^2 - |E(z)|^2\} \\ &= \sum_n A_n^2 (1 + \sigma^2) - \sum_n A_n^2 \Phi^2(1), \end{aligned} \quad (\text{A15})$$

$$E\{(G)^2\} = \sum_{n,m} \Phi^2(1) e^{j(n+m)\mu} + \sum_n A_n^2 (1 + \sigma^2) \Phi(z) e^{j2n\mu}, \quad (\text{A16})$$

$$E\{[G - E(G)]^2\} = E\{(G)^2\} - [E(G)]^2$$

$$= [(1 + \sigma^2) \Phi(2) - \Phi^2(1)] e^{j2n\mu},$$

$$\sigma_1^2 = \frac{1}{2} [1 + \sigma^2 - \Phi^2(1)] \sum_n A_n^2 + \frac{1}{2} [(1 + \sigma^2) \Phi(2) - \Phi^2(1)] \sum_n A_n^2 \cos 2n\mu, \quad (\text{A17})$$

$$\sigma_2^2 = \frac{1}{2} [1 + \sigma^2 - \Phi^2(1)] \sum_n A_n^2 - \frac{1}{2} [(1 + \sigma^2) \Phi(2) - \Phi^2(1)] \sum_n A_n^2 \cos 2n\mu, \quad (\text{A18})$$

and

$$\sigma_{12} = \frac{1}{2} [(1 + \sigma^2) \Phi(2) - \Phi^2(1)] \sum_n A_n^2 \sin 2n\mu. \quad (\text{A19})$$

## Appendix B

### PROOF THAT THE ILLUMINATION FUNCTION IS BOUNDED

Cauchy's inequality is given by [B1]

$$\left( \sum_{i=1}^N X_i Y_i \right)^2 \leq \left( \sum_{i=1}^N X_i^2 \right) \left( \sum_{i=1}^N Y_i^2 \right).$$

Let  $Y_i = 1$ , then

$$\left( \sum_i X_i \right)^2 \leq \left( \sum_i X_i^2 \right) N,$$

or

$$\frac{1}{N} \leq \frac{\sum_i X_i^2}{\left( \sum_i X_i \right)^2}.$$

When  $X_i = 1$ ,

$$\frac{\sum X_i^2}{\left( \sum X_i \right)^2} = \frac{1}{N},$$

therefore

$$\frac{\sum X_i^2}{\left( \sum X_i \right)^2}$$

is bounded.

#### REFERENCE

B1. E.F. Beckenbach and R. Bellman, *Inequalities*, Springer-Verlag, Berlin, 1971, p. 2.

## Appendix C

## DERIVATION OF VARIANCES FOR A PLANAR ARRAY

For the noncorrelated case,

$$G(\mu, \nu) = \sum_n \sum_m (1 + \delta_{nm}) \exp(j\phi_{nm}) \cdot \exp[j(m\mu + n\nu)] A_{nm}, \quad (C1)$$

$$E[G(\mu, \nu)] = \sum_n \sum_m \Phi_{nm}(1) A_{nm} \exp[j(m\mu + n\nu)], \quad (C2)$$

$$|G(\mu, \nu)|^2 = \sum_n \sum_m \sum_r \sum_s A_{nm} A_{rs} (1 + \delta_{nm}) (1 + \delta_{rs}) \exp[j(\phi_{nm} - \phi_{rs})] \cdot \exp\{j[(m-s)\mu + (n-r)\nu]\}, \quad (C3)$$

$$E[|G(\mu, \nu)|^2] = \sum_n \sum_m \sum_r \sum_s A_{nm} A_{rs} \Phi_{nm}^2(1) \exp\{j[(m-s)\mu + (n-r)\nu]\} + \sum_n \sum_m A_{nm}^2 (1 + \sigma_{nm}^2), \quad (C4)$$

$$|E[G(\mu, \nu)]|^2 = \sum_n \sum_m \sum_r \sum_s \Phi_{nm}^2(1) A_{nm} A_{rs} \exp\{j[(m-s)\mu + (n-r)\nu]\}, \quad (C5)$$

$$\begin{aligned} \sigma_1^2 + \sigma_2^2 &= E[|G(\mu, \nu)|^2] - |E[G(\mu, \nu)]|^2 \\ &= \sum_n \sum_m [1 + \sigma_{nm}^2 - \Phi_{nm}^2(1)], \end{aligned} \quad (C6)$$

$$[G(\mu, \nu)] = \sum_n \sum_m \sum_r \sum_s (1 + \delta_{nm}) (1 + \delta_{rs}) \exp[j(\phi_{nm} + \phi_{rs})] \exp[j(m+s)\mu + (n+r)\nu], \quad (C7)$$

$$\begin{aligned} E\{|G(\mu, \nu)|^2\} &= \sum_n \sum_m \sum_r \sum_s A_{nm} A_{rs} \Phi_{nm}(1) \exp[j(m+s)\mu + (n+r)\nu] \\ &\quad + \sum_n \sum_m (1 + \sigma_{nm}^2) \Phi_{nm}(2) A_{nm}^2 \exp[j(2m\mu + 2n\nu)], \end{aligned} \quad (C8)$$

$$\{E[G(\mu, \nu)]\}^2 = \sum_n \sum_m \sum_r \sum_s A_{nm} A_{rs} \Phi_{nm}^2(1) \exp[j(m+s)\mu + (n+r)\nu], \quad (C9)$$

$$\sigma_1^2 - \sigma_2^2 = \sum_n \sum_m [(1 + \sigma_{nm}^2) \Phi_{nm}(2) - \Phi_{nm}^2(1)] A_{nm}^2 \cos(2m\mu + 2n\nu), \quad (C10)$$

$$\sigma_{12} = \frac{1}{2} \sum_n \sum_m [(1 + \sigma_{nm}^2) \Phi_{nm}(2) - \Phi_{nm}^2(1)] A_{nm}^2 \sin(2m\mu + 2n\nu), \quad (C11)$$

$$\sigma_1^2 = \frac{1}{2} \sum_n \sum_m [C_{nm} + D_{nm} \cos(2m\mu + 2n\nu)] \quad (C12a)$$

and

$$\sigma_2^2 = \frac{1}{2} \sum_n \sum_m [C_{nm} - D_{nm} \cos(2m\mu + 2n\nu)] \quad (C12b)$$

where

$$C = [1 + \sigma_{nm}^2 - \Phi_{nm}^2(1)] A_{nm}^2 \quad (C12c)$$

and

$$D = [(1 + \sigma_{nm}^2) \Phi_{nm}(2) - \Phi_{nm}^2(1)] A_{nm}^2. \quad (C12d)$$

For the case of correlated errors,

$$G(\mu, \nu) = \sum_n (1 + \delta_n) \exp(j\phi_n) \sum_m (1 + \delta_{nm}) \exp(j\phi_{nm}) A_{nm} \exp[j(m\mu + n\nu)], \quad (C13)$$

$$E[G(\mu, \nu)] = \sum_n \sum_m \Phi_n(1) \Phi_{nm}(1) A_{nm} \exp[j(m\mu + n\nu)], \quad (C14)$$

$$|G(\mu, \nu)|^2 = \sum_n \sum_r (1 + \delta_n) (1 + \delta_r) \exp[j(\phi_n - \phi_r)] \sum_m \sum_s (1 + \delta_{nm}) (1 + \delta_{rs}) \cdot A_{nm} A_{rs} \exp[j(\phi_{nm} - \phi_{rs})] \exp[j(m-s)\mu + (n-r)\nu], \quad (C15)$$

$$E[|G(\mu, \nu)|^2] = \sum_n \sum_r r \Phi_n^2(1) \sum_{\substack{m \\ m \neq s}} \sum_s \Phi_{nm}^2(1) A_{nm} A_{rs} \exp[j(m-s)\mu + (n-r)\nu] + \sum_n (1 + \sigma_n^2) \sum_{\substack{m \\ m \neq s}} \sum_s \Phi_{nm}^2(1) A_{nm} A_{ns} \exp[j(m-s)\mu] + \sum_{\substack{n \\ n \neq r}} \sum_r \Phi_n^2(1) \cdot \sum_m \Phi_{nm}^2(1) A_{nm} A_{rm} \exp[j(n-r)\nu] + \sum_n \sum_m (1 + \sigma_n^2) (1 + \sigma_{nm}^2) A_{nm}^2, \quad (C16)$$

$$|E[G(\mu, \nu)]|^2 = \sum_n \sum_m \sum_r \sum_s A_{nm} A_{rs} \Phi_n^2(1) \Phi_{nm}^2(1) A_{nm} A_{rs} \exp[j[(m-s)\mu + (n-r)\nu]], \quad (C17)$$

$$\sigma_1^2 + \sigma_2^2 = \sum_n \sum_m [(1 + \sigma_n^2) (1 + \sigma_{nm}^2) - \Phi_n^2(1) \Phi_{nm}^2(1)] A_{nm}^2 + \sum_n [(1 + \sigma_n^2) - \Phi_n^2(1)] \Phi_{nm}^2(1) \sum_m \sum_s A_{nm} A_{ns} \cos(m-s)\mu \quad (C18)$$

$$|G(\mu, \nu)|^2 = \sum_n \sum_r (1 + \delta_n) (1 + \delta_r) \exp[j(\phi_n + \phi_r)] \sum_m \sum_s (1 + \delta_{nm}) (1 + \delta_{rs}) \cdot \exp[j(\phi_{nm} + \phi_{rs})] A_{nm} A_{rs} \exp\{j[(m+s)\mu + (n+r)\nu]\}, \quad (C19)$$

$$E[|G(\mu, \nu)|^2] = \sum_{\substack{n \\ n \neq r}} \sum_r \Phi_n^2(1) \sum_{\substack{m \\ m \neq s}} \sum_s \Phi_{nm}^2(1) A_{nm} A_{rs} \exp\{j[(m+s)\mu + (n+r)\nu]\} + \sum_n (1 + \sigma_n^2) \Phi_n(2) \sum_{\substack{m \\ m \neq s}} \sum_s \Phi_{nm}^2 A_{nm} A_{ns} \exp\{j[(m+s)\mu + 2n\nu]\} + \sum_{\substack{n \\ n \neq r}} \sum_r \Phi_n^2(1) \sum_m \Phi_{nm}^2 A_{nm} A_{rm} \exp[j(2m\mu + (n+r)\nu)] + \sum_n \sum_m [(1 + \sigma_n^2) (1 + \sigma_{nm}^2) \Phi_n(2) \Phi_{nm}(2)] A_{nm}^2 \exp[j(2m\mu + 2n\nu)], \quad (C20)$$

$$\{E[G(\mu, \nu)]\}^2 = \sum_n \sum_v \sum_m \sum_s \Phi_n^2(1) \Phi_{nm}^2(1) A_{nm} A_{rs} \exp\{j[(m+s)\mu + (n+r)\nu]\}, \quad (C21)$$

$$\sigma_1^2 - \sigma_2^2 = \sum_n \sum_m [(1 + \sigma_n^2) (1 + \sigma_{nm}^2) \Phi_n(2) \Phi_{nm}(2) - \Phi_n^2(1) \Phi_{nm}^2(1)] A_{nm} \cos(2m\mu + 2n\nu) + \sum_n \sum_m \sum_s [(1 + \sigma_n^2) \Phi_n(2) - \Phi_{nm}^2(1)] \Phi_{nm}^2 A_{nm} A_{ns} \cdot \cos[(m+s)\mu + 2n\nu], \quad (C22)$$

$$\begin{aligned}
\sigma_{12} = & \frac{1}{2} \sum_n \sum_m [(1 + \sigma_n^2) (1 + \sigma_{nm}^2) \Phi_n(2) \Phi_{nm}(2) - \Phi_n^2(1) \Phi_{nm}^2(1)] \\
& \cdot A_{nm}^2 \sin(2m\mu + 2n\nu) \\
& + \frac{1}{2} \sum_n \sum_m \sum_s [(1 + \sigma_n^2) \Phi_n(2) - \Phi_n^2(1)] \\
& \cdot \Phi_{nm}^2(1) A_{nm} A_{ns} \sin[(m + s)\mu + 2n\nu], \tag{C23}
\end{aligned}$$

$$\sigma_1^2 = E + F \tag{C23a}$$

and

$$\sigma_2^2 = E - F, \tag{C23b}$$

where

$$\begin{aligned}
E = & \frac{1}{2} \sum_n \sum_m [(1 + \sigma_n^2) (1 + \sigma_{nm}^2) - \Phi_n^2(1) \Phi_{nm}^2(1)] A_{nm}^2 \\
& + \frac{1}{2} \sum_n [(1 + \sigma_n^2) - \Phi_n^2(1)] \Phi_{nm}^2(1) \sum_m \sum_s A_{nm} A_{ns} \cos(m - s)\mu \tag{C23c}
\end{aligned}$$

and

$$\begin{aligned}
F = & \frac{1}{2} \sum_n \sum_m [(1 + \sigma_n^2) (1 + \sigma_{nm}^2) \Phi_n(2) \Phi_{nm}(2) - \Phi_n^2(1) \Phi_{nm}^2(1)] A_{nm}^2 \cos(2m\mu + 2n\nu) \\
& + \frac{1}{2} \sum_n \sum_m \sum_s [(1 + \sigma_n^2) \Phi_n(2) - \Phi_n^2(1)] \Phi_{nm}^2(1) A_{nm} A_{ns} \cos[(m + s)\mu + 2n\nu]. \tag{C23d}
\end{aligned}$$